Available online at www.sciencedirect.com
ScienceDirect
International Journal of Pharmaceutics 334 (2007) 179–189
INTERNATIONAL JOURNAL OF PHARMACEUTICS
www.elsevier.com/locate/ijpharm

Pharmaceutical Nanotechnology

Investigation of surface-modified solid lipid nanocontainers formulated with a heterolipid-templated homolipid

A.A. Attama [a,b,*], C.C. Müller-Goymann [a]

[a] *Institut für Pharmazeutische Technologie, Technische Universität Carolo-Wilhelmina zu Braunschweig, Mendelssohnstraße 1, D-38106 Braunschweig, Germany*
[b] *Department of Pharmaceutics, University of Nigeria, Nsukka 410001, Enugu State, Nigeria*

Received 18 January 2006; received in revised form 9 October 2006; accepted 17 October 2006
Available online 28 October 2006

Abstract

There is increasing interest in the search for improved drug delivery systems with greater versatility. Consequently, many drug delivery systems have been studied. In this study, surface-modified lipid nanocontainers were formulated with a homolipid from *Capra hircus* (goat fat) templated with a heterolipid (Phospholipon 90G®) which was also the surface modifier. The solid lipid nanocontainers (SLN) were formulated by hot high pressure homogenisation using increasing concentrations of polysorbate 80 as the mobile surfactant. Prior to SLN preparation, the templated homolipid was formulated by fusion to obtain a homogeneous lipid matrix, which was characterized using differential scanning calorimetry (DSC), polarized light microscopy (PLM) and wide angle X-ray diffraction (WAXD) to obtain its thermal and crystal characteristics. Isothermal heat conduction microcalorimetry (IMC) and freeze-fracture transmission electron microscopy (FFTEM) studies were carried out on the templated homolipid and SLN containing 1.0% (w/w) of polysorbate 80 to study their in situ crystallization kinetics and morphology, respectively. The formulated SLN were also subjected to time-resolved DSC, WAXD and particle size analyses for one month. The thermal and crystal characteristics were compared with those of the bulk lipid matrix (templated homolipid). Result of the particle size analysis indicated that the particles size remained roughly within the lower nanometer range after one month. FFTEM micrograph of the lipid matrices revealed lamellar sheets for Phospholipon 90G® and layered triglyceride structures for the homolipid and Phospholipon 90G®-templated homolipid. FFTEM micrograph of SLN revealed anisometric structures. PLM of the templated homolipid did not show, but goat fat (homolipid) alone showed slight growth in crystals with time. WAXD and DSC studies revealed minor increase in crystallinity of the new lipid matrix after one month and DSC also detected templation of homolipid by the heterolipid noted by the disappearance of the lower melting peak of the homolipid. However, for the SLN, WAXD results showed low crystalline particles while DSC only showed a very little endothermic process after one month of storage at 20°C. The implication of this finding is that progression of the SLN to highly ordered particles over time would not occur. This will be favourable for any incorporated drug as drug expulsion, due to increase in crystallinity, will not occur. Result obtained from analysis of the isothermal crystallization exotherms indicated that the templated homolipid and SLN1 containing 1.0% polysorbate 80 possess similar nucleation mechanisms and growth dimensions different from the pure homolipid. The SLN containing 0.5 and 1.0% polysorbate 80 possessed good properties and could prove to be good delivery systems for drugs for parenteral or ocular administration. The result of this study also shows a method of improving natural lipids for use in particulate drug delivery systems.

Keywords: Homolipid; Heterolipid; Templation; Lipid nanocontainers; Surface modification; Crystallinity; In situ crystallization; Drug delivery

1. Introduction

During the past decade, there has been increasing focus on the search for improved drug delivery systems with greater versatility. Delivery systems such as polymers, liposomes, nano- and microparticles, bacterial and cellular ghosts have been studied (Cortesi and Nastruzzi, 2001). Solid lipid nanoparticulate drug delivery system has been proposed as a promising alternative colloidal drug delivery system to liposomes and polymer nanoparticles (Siekmann and Westesen, 1992). Solid lipid nanoparticles/nanocontainers (SLN) are an aqueous colloidal dispersion of particles composed of biodegradable lipids and drug, in the sub micron size range. General features of SLN are their good tolerability, that is, low

* Corresponding author. Tel.: +234 42 771911; fax: +234 42 771709.
E-mail address: aaattama@yahoo.com (A.A. Attama).

0378-5173/$ – see front matter © 2006 Elsevier B.V. All rights reserved.
doi:10.1016/j.ijpharm.2006.10.032

systemic toxicity and low cytotoxicity due to their composition of physiological, biocompatible and biodegradable lipid, and pharmaceutically acceptable surfactants (Westesen et al., 1997; Müller et al., 2000). SLN are suitable for the incorporation of lipophilic, hydrophilic and poorly water-soluble drugs within the lipid matrix in considerable amounts (Schubert and Müller-Goymann, 2003; Hou et al., 2003). This drug delivery system combines the advantages of colloidal lipid emulsions with advantages of particles with a solid monolithic matrix, but may be limited by low drug payload capability. Such SLN are expected to release incorporated drugs more slowly than conventional, more fluid type-colloidal lipid drug carriers since a solid matrix binds the drug molecules more tightly and may also improve the stability of sensitive drugs against decomposition. A slow release is advantageous, for example, for intravenous drug targeting where it is important that the incorporated drug should remain bound until it reaches its target. Cells of the reticuloendothelial system (RES), the liver or the brain could easily be reached using SLN. Rapid escape of nanoparticles from the endolysosomal compartment to the cytoplasmic compartment has been demonstrated (Panyam et al., 2002). Thus, nanoparticles could be an effective drug delivery mechanism for drugs whose targets are cytoplasmic (Panyam and Labhasetwar, 2004).

A variety of emulsifiers has been used for the preparation of SLN dispersions including phospholipids, bile salts, poloxamers and other ionic and non-ionic surfactants. Stabilization of SLN with phospholipids and an additional surfactant rather than with a single surfactant frequently yields dispersions with a more homogeneous appearance and lower tendency to form macroscopic particles (Westesen et al., 2003). This approach has been adopted in our laboratory and has led to the development of surface-modified SLN containing high amount of lecithin (Schubert et al., 2005; Schubert and Müller-Goymann, 2005). Surface-modified SLN have several advantages. Biologically important molecules (and drugs) may be anchored to colloidal particle surface and such nanoparticles have potential applications in bio-diagnosis and immunoassay, and as luminescent bio-conjugates for ultra-sensitive biological detection (Sastry, 2000). In addition, surface modification also enables electrostatic stabilization of colloidal particles, especially when synthesis of the colloidal particles is carried out in aqueous medium. Concentration of phospholipid with optimum performance in stabilizing SLN has been established in our laboratory with respect to hard fats (Schubert et al., 2005; Schubert and Müller-Goymann, 2005). The homolipid (goat fat) used in this study has been found to perform well as a drug delivery matrix (Attama et al., 2003; Attama and Nkemnele, 2005). Based on the above premises, it was the objective of this study to formulate and characterize nanocontainers with a homolipid (goat fat) templated with Phospholipon 90G® (lecithin), a heterolipid, with a view to applying them as nanoparticles for parenteral and ocular drug delivery, and for targeted drug delivery systems. Heterolipids contain other functional groups in addition to fatty acid moiety (Stuchlík and Žák, 2001). The formulated SLN were subjected to several analytical techniques including static light scattering for particle size measurement, differential scanning calorimetry (DSC), wide angle X-ray diffraction (WAXD), freeze-fracture transmission electron microscopy (FFTEM) and isothermal heat conduction microcalorimetry (IMC) performed in parallel to obtain information on the colloidal lipid dispersion.

2. Materials and methods

2.1. Materials

Phospholipon 90G®, provided by Phospholipid GmbH (Köln, Germany), is a purified, deoiled and granulated soy lecithin with a phosphatidylcholine content of at least 90%. Thimerosal (Synochem, Germany), sorbitol (Caesar & Loretz, Germany) and polysorbate 80 (Tween 80®) (Across Organics, Germany) were used as procured from their manufacturers without further purification. Homolipid (goat fat) was obtained from a batch processed in our laboratory according to earlier procedure (Attama et al., 2003; Attama and Nkemnele, 2005). Bidistilled water was used for all formulations.

2.2. Formulation of the templated homolipid

The lipid matrix corresponding to 30% (w/w) of Phospholipon 90G® in the homolipid was prepared by fusion. The lipids were weighed with an electronic balance (Type L2200P-xD2, Sartorius AG Göttingen, Germany) and melted together at 70 °C on a hot plate (RCT basic, IKA® Staufen Germany) and stirred with a Teflon coated magnetic stirring bar until a yellow transparent solution was obtained and continued until solidification.

2.3. Formulation of solid lipid nanocontainers

The nanocontainers were formulated following the formula below, and correspond to SLN1, SLN2, SLN3 and SLN4 with 1.0, 0.5, 0.1 and 0.0% (w/w) of polysorbate 80, respectively.

	% (w/w)
Lipid matrix (templated homolipid)	5.0
Polysorbate 80	0.0, 0.1, 0.5 and 1.0
Thimerosal	0.005
Sorbitol	4.0
Bidistilled water qs ad	100

The hot homogenisation technique was adopted. In each case, the lipid matrix was melted at 70 °C and the bidistilled water containing polysorbate 80, thimerosal and sorbitol was added to the molten lipid matrix at the same temperature, mixed very well with a Teflon coated magnetic stirring bar and vigorously dispersed with Ultra-Turrax (T25 basic, IKA® Staufen Germany) at 24,000 rpm for 5 min to produce the hot primary emulsion. The hot primary emulsion at 60 °C was immediately passed through a heated high pressure homogeniser (EmulsiFlex-C5, Avestin Canada) at a pressure of 1000 bars for 20 cycles to produce the nanocontainers. The nanocontainers were collected in a hot container and thereafter allowed to recrystallize at room temperature.

2.4. Particle sizing

Particle size distributions were measured using a multi-wavelength laser diffraction particle size analyser (Coulter LS13 320, Beckman Coulter, USA), which operates on the principles of Fraunhofer and Mie theories of diffraction and uses polarization intensity differential scattering (PIDS) technology. Prior to measurement, the samples were diluted with demineralised water to appropriate PIDS obscurity of not less than 40%. Data were collected during 60 s and further analysed using the volume distribution diameter 50% ($d_{50\%}$), 75% ($d_{75\%}$) and 90% ($d_{90\%}$). For instance, $d_{90\%}$ means that 90% of the particles are below this value. Size distribution by volume were calculated by applying an optical module created by the instrument software. Values reported are the average of three successive 60 s runs of different samples, measured 24 h, one week and one month after SLN preparation.

2.5. Wide angle X-ray diffraction

WAXD was used to characterize the crystal character of the lipid matrix and the formulated SLN. X-ray reflections due to crystalline lipids appear above the amorphous background of non-crystalline lipids. Wide angle X-ray studies were done on the templated homolipid and the formulated SLN using an X-ray generator (PW3040/60 X'Pert PRO, Fabr. DY2171, PANalytical Netherlands) connected to the tube (PW3373/00 DK 147726 Cu LFF) copper anode which delivered X-ray of wavelength $\lambda = 0.1542$ nm, at a high voltage of 40 kV and an anode current of 25 mA. WAXD measurements were taken with a Goniometer (PW3050/60 MPD-System, PANalytical Netherlands) from 3.0° to 33.0° in 0.015° steps (1 s per step). The interlayer spacing was calculated from the scattering angle θ, using Bragg's equation (Eq. (1)).

$$n\lambda = 2d \sin\theta \quad (1)$$

where λ is the wavelength of the incident X-ray beam, n is a positive integer which describes the order of the interference and the parameter d, otherwise called the interlayer spacing is the separation between a particular set of planes of the crystal lattice structure. WAXD diffractograms were obtained 24 h, one week and one month after lipid matrix and, 24 h and one month after SLN preparation.

2.6. Differential scanning calorimetry

Thermal behaviour of the new lipid matrix and the degree of crystallinity of the formulated SLN were determined with a calorimeter (DSC 220C) connected to a disc station (5200H, Seiko, Tokyo Japan). Approximately 5 mg of the new lipid matrix or SLN was weighed into an aluminium pan and sealed hermetically, and the thermal behaviour determined against an empty pan in the range of 20–125°C at a heating rate of 5°C min^{-1}. DSC thermograms were recorded 24 h, one week and one month after lipid matrix and SLN preparation. Transition temperatures were determined from the endothermic peak minimum temperatures while enthalpies were obtained by integration of the endotherms within the range of 22–57°C using linear baselines.

2.7. Polarized light microscopy (PLM)

Micrographs of crystallizing lipids and the new lipid matrix were examined with a Zeiss Type III photomicroscope (Model No. SIP 48560, Oberkochen, West Germany) using cross polarizers and a wavelength (λ) plate. The polarizer and analyser were adjusted to crossed positions to yield the greatest contrast between the crystals and the background. The micrographs of statically crystallized lipid matrices at 25°C were digitalized after 24 h, one and four weeks with a digital camera (Olympus DP12, Japan) attached to the photomicroscope.

2.8. Freeze-fracture transmission electron microscopy

The FFTEM of the pure lipids, the new lipid matrix and the SLN containing 1.0% (w/w) of polysorbate 80 (SLN1) was done to further study their morphologies. In each case, the sample was shock-frozen in melting nitrogen at 63 K between two flat gold holders. The frozen sample was fractured at 173 K in a BAF 400 instrument (Balzers, D-Wiesbaden, Germany) and then shadowed with platinum/carbon (2 nm) at 45° and with pure carbon at 90° for replica stabilization. After cleaning with chloroform–methanol mixture (1:1), the replicas on uncoated grids were fixed unto a sample holder and placed in the vacuum chamber of a transmission electron microscope (Leo 922, Leo D-Oberkochen Germany), and viewed under low vacuum at 200 kV.

2.9. Isothermal heat conduction microcalorimetry

To determine the in situ crystallization kinetics of the lipid matrix or SLN, a 2277 Thermal Activity Monitor® (TAM, Thermometric AB, Jarfalla Sweden) was used. Two calorimeter units were installed and run concurrently. A 300 mg quantity of the molten homolipid or templated homolipid (at 70 °C) was weighed into 3 ml glass ampoule and equilibrated for 30 min at 20 °C, and then the heat flow measured at the range of −3000 to 3000 μW. Heat flow signals were monitored by the Digitam Software (Thermometric AB, Jarfalla Sweden). Data obtained from the IMC measurements were thereafter analysed to determine the isothermal crystallization kinetics of the lipid matrix. During crystallization from a melt, the extent of crystallization is usually thought to be related to time through an equation developed by Avrami, and may be expressed in the following form (Avrami, 1939, 1940):

$$1 - X_t = \exp(-kt^n) \quad (2)$$

where X_t represents the degree of crystallinity at time t, k is the growth rate constant of isothermal crystallization and the exponent n, represents the nucleation mechanism and growth dimension. The value of n can be any positive integer between 1 and 4. For the IMC studies of SLN, 2 g of the nanocontainers

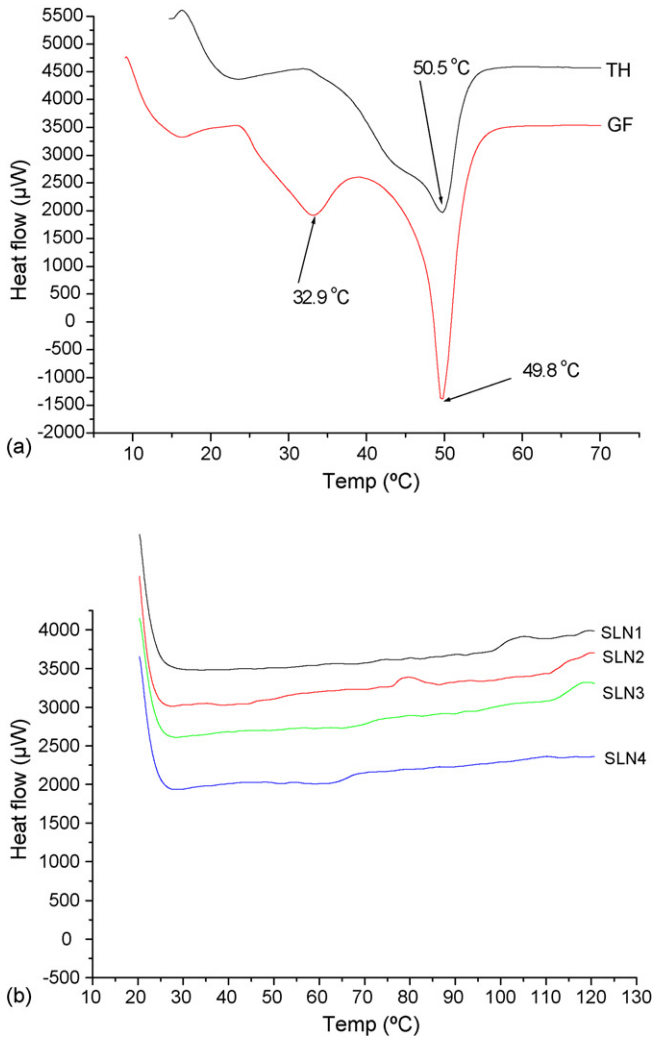

Fig. 1. (a) DSC traces obtained for the lipid matrices after one month: homolipid (GF), templated homolipid (TH). (b) DSC traces obtained for the nanoparticles after one month: SLN1, SLN2, SLN3 and SLN4 represent SLN that contained 1.0, 0.5, 0.1 and 0.0% (w/w) polysorbate 80, respectively.

were equilibrated at 20 °C for 30 min after preparation before measurement to dissipate excess heat arising from the high formulation temperature.

3. Results and discussion

3.1. Differential scanning calorimetry

DSC is an important tool to investigate the melting and recrystallization behaviour or the degree of crystallinity of crystalline materials. The thermograms presented in Fig. 1a revealed that the melting peak of the new lipid matrix was 50.5 ± 0.3 °C after one month while values of 50.6 ± 0.2 °C and 50.9 ± 0.3 °C were obtained after 24 h and one week, respectively (thermograms not shown). There was also a slight drop in enthalpy, from 61.9 ± 1.7 mJ/mg after one day to 53.6 ± 1.4 mJ/mg after one month. This signify a minor decrease in crystallinity. The thermotropic phase behaviour of a lipid matrix system is highly affected by the presence of guest molecules, and the related thermodynamic variables (melting temperature and enthalpy changes) depend on the nature of the interaction between the constituents. Phospholipids contain two fatty acid chains (hydrophobic tail) usually with even carbon number. The fatty acids may be saturated or unsaturated and their configuration is nearly always cis. Phospholipids are therefore, non-homogeneous materials with mainly saturated acyl chains at the sn-1 position and unsaturated acyl chain at the sn-2 position (Stuchlík and Žák, 2001). Phospholipon 90G® used in this study, is a purified, deoiled and granulated soy lecithin with a phosphatidylcholine content of at least 90% and an HLB value of 10, and has been found to contain stearic acid and palmitic acid, which are saturated fatty acids (Stuchlík and Žák, 2001; Ghyczy and Niemann, 1992). These fatty acids are also present in the homolipid. The location of fatty acids in the homolipid (goat fat) triglycerides as with other animal fats, has been shown not to be homogeneous, which resulted in the observed two endothermic peaks for goat fat (Attama and Müller-Goymann, 2006). Thus, the addition of Phospholipon 90G® to the homolipid resulted in a greater ordering of the fatty acid positions in its triglycerides by a templating mechanism since saturated fatty acids pack better due to increased Van der Waals attraction and better chain alignment as there is no dimensional deformation due to unsaturation. This resulted in crystallization enhancing effect on this lipid matrix. The thermograms of the new lipid matrix did not have two endothermic peaks at all stages of the study as originally present in pure homolipid (Fig. 1a). The templating effect led to the disappearance of the lower melting peak characteristic of goat fat which usually occurs around 32.9 °C (Attama and Müller-Goymann, 2006). The disappearance of this lower melting peak of goat fat on addition of Phospholipon 90G® resulted in a highly cooperative thermal phase transition. The interesting thing here is that the templating effect did not significantly affect the higher melting peak of goat fat, but affected the total enthalpy of the endothermic process. The higher melting peak of pure goat fat occurs around 49.8 °C against 50.5 ± 0.3 °C for the Phospholipon 90G®-templated goat fat after one month. The enthalpy of pure goat fat was 97.2 ± 2.5 mJ/mg as against 53.6 ± 1.4 mJ/mg obtained for the templated goat fat. Referring to a 70% (w/w) content of goat fat in the templated homolipid, the decrease in enthalpy is significantly higher ($p < 0.05$) than expected. This means that the templation did not lead to increase in crystallinity. It is envisaged that drugs could be trapped in the crevices or between the fatty acids before and/or during templation.

DSC was also used to investigate the crystalline status of the SLN. The thermograms of the SLN are presented in Fig. 1b, representing the thermograms obtained after one month. There was virtually no definite thermal event in the SLN compared with the bulk matrix which had endothermic transition at 50.5 ± 0.3 °C (Fig. 1a). The enthalpies and peaks of these SLN transitions could not be obtained. However, a critical look at the endotherms showed that none of the wavering thermal events had a transition signal close to 50.5 ± 0.3 °C recorded for the bulk lipid matrix. Recrystallization of lipid nanoparticles may be different from that of the bulk lipid. The fact that almost no thermal event occurred after one month shows that the SLN exist as

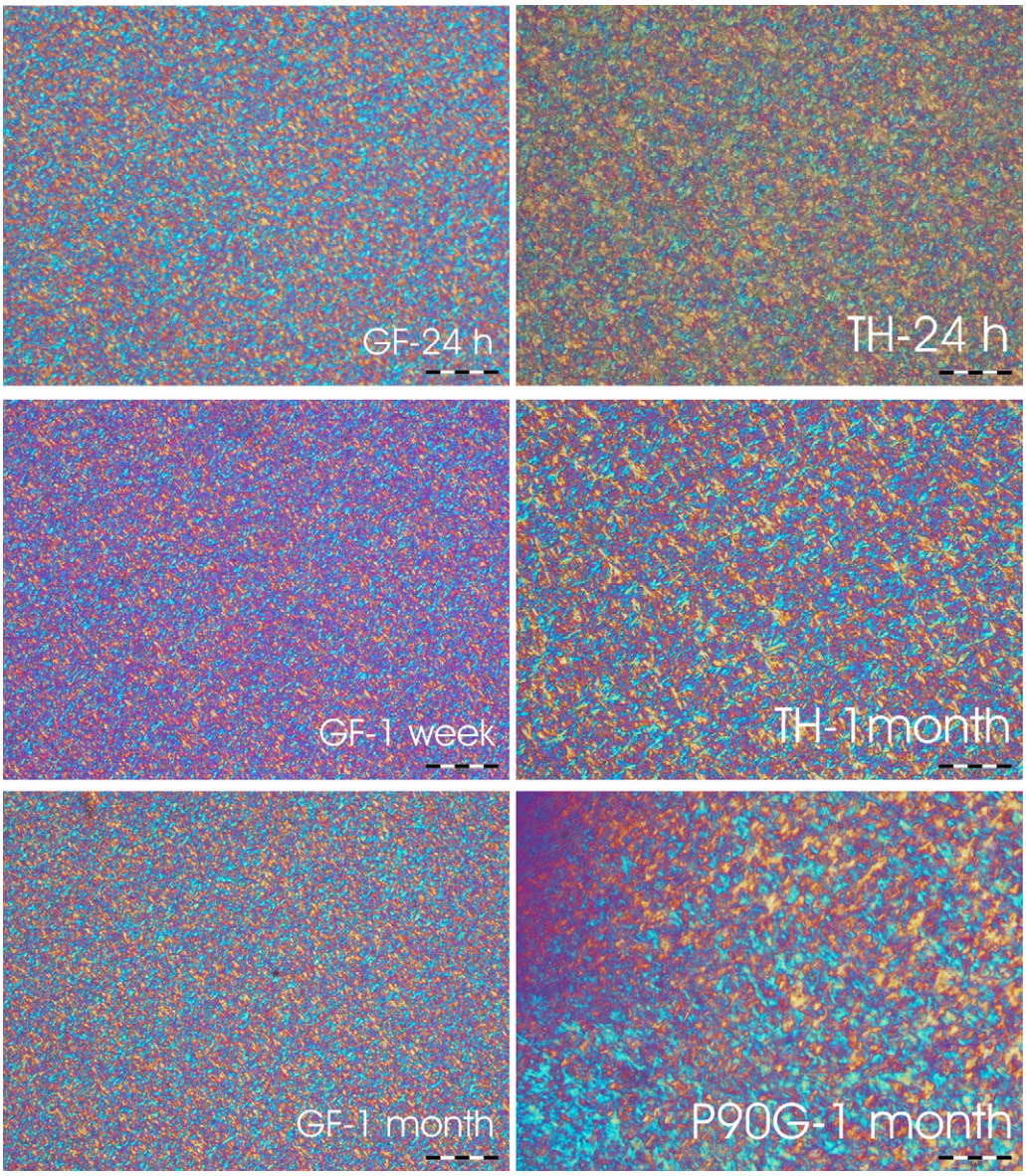

Fig. 2. Polarized light micrographs of the lipid matrices: templated homolipid (TH) after 24 h and one month (TH-24 h and TH-1 month), Phospholipon 90G® after one month (P90G-1 month), homolipid after 24 h, one week and one month (GF-24 h, GF-1 week and GF-1 month, respectively). Bar represents 100 μm.

less ordered crystals or amorphous state, the melt of which did not require or just required less energy than the crystalline lipid matrix which needed to overcome lattice force (Hou et al., 2003). Therefore, it is reasonable to state that the lipid within the particulate nanocontainers were in a less ordered arrangement compared with the bulk lipid matrix as detected by DSC. This less ordered arrangement will favour drug loading (Radtke et al., 2005). Absence of thermal event may also be attributed to the low particle size of the SLN. DSC result shows addition of P90G to goat fat improved properties of SLN formulated therefrom, and this has widened the applicability of goat fat in drug delivery. This SLN formulated from templated goat fat will find use in parenteral, ocular and other drug delivery systems requiring small particle size, narrow particle size distribution and particle size stability as in vivo tolerability of natural lipids is higher than semi-synthetic lipids.

3.2. Polarized light microscopy

This is a useful tool in visualizing the static crystallization of lipid matrices, but is limited to the microlevel only. Consequently, only the lipid matrix was studied using PLM. The PLM micrographs are presented in Fig. 2. In the templated homolipid, very little difference was shown by the coarser texture observed after one month, further attesting that crystallization was almost complete within 24 h. No difference was also observed for Phospholipon 90G® alone between one day and one month. However, for goat fat alone, there was a slight difference in matrix texture observed after one week and one month compared with 24 h. Crystallization is a random process and the crystallization behaviour of the lipid matrix was not equal within all parts of the laminates. This means that Phospholipon 90G® rather than delaying the crystallization of goat fat, enhanced it attesting

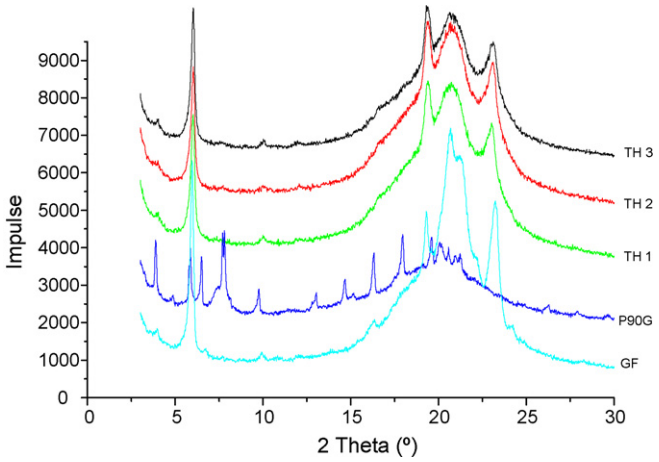

Fig. 3. WAXD diffractograms of the lipid matrix: GF (homolipid), P90G (Phospholipon 90G®) and TH1, TH2 and TH3 (templated homolipid after 24 h, one week and one month, respectively).

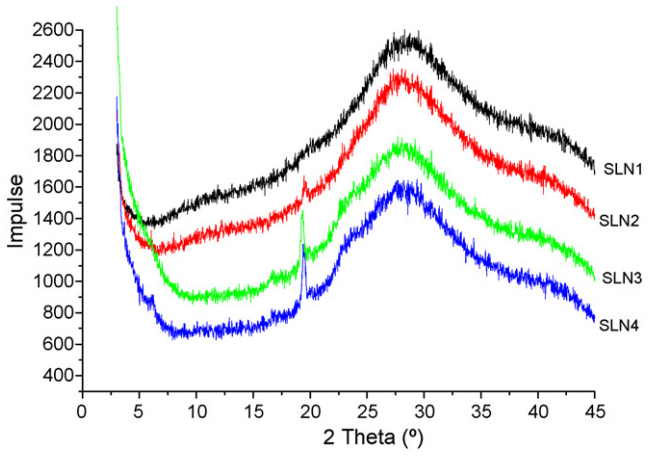

Fig. 4. WAXD diffractograms of the nanoparticles obtained after one month: SLN1, SLN2, SLN3 and SLN4 containing 1.0, 0.5, 0.1 and 0.0% (w/w) polysorbate 80, respectively.

further to the earlier result presented on templation. Saturated phospholipids have been shown to enhance crystallization but delay polymorphic transition in triglycerides (Bunjes and Koch, 2005).

3.3. Wide angle X-ray diffraction

To study the crystallinity of the lipids, the new lipid matrix (templated homolipid) and SLN, WAXD studies were performed. WAXD diffractograms of the lipid matrices obtained after 24 h, one week and one month are presented in Fig. 3, while the calculated interlayer spacings obtained from WAXD measurements of the templated homolipid after 24 h, one week and one month are presented in Table 1. The templated homolipid showed very high intensity reflections at $2\theta = 6.0°$, $d = 14.73$ Å; $2\theta = 19.4°$, $d = 4.58$ Å; $2\theta = 20.7°$, $d = 4.29$ Å and $2\theta = 23.0°$ $d = 3.87$ Å after one day of preparation. The first three reflections remained unchanged after one week and one month, while the last reflection shifted to $2\theta = 23.1°$ $d = 3.85$ Å after one week but remained unchanged after one month (Table 1, Fig. 3). Two weak reflections at $2\theta = 4.0°$, $d = 22.09$ Å and $2\theta = 10.0°$ $d = 8.85$ Å which appeared after one day also persisted at the same positions and intensities after one month.

Reflections due to templated homolipid and pure goat fat occurred almost at similar positions between $2\theta = 18°$ and 25°, while Phospholipon 90G® had reflections mostly between $2\theta = 6°$ and 22°. Stable form of goat fat presents characteristic reflections of high intensity at $2\theta = 6.0°$, $d = 14.73$ Å; $2\theta = 19.3°$, $d = 4.60$ Å; $2\theta = 20.7°$, $d = 4.29$ Å; $2\theta = 21.3°$, $d = 4.17$ Å and $2\theta = 23.2°$, $d = 3.83$ Å and a very weak reflection at $2\theta = 10.0°$ $d = 8.85$ Å. This indicates that as a result of templation of the homolipid (goat fat) by Phospholipon 90G®, the new lipid matrix crystallized into stable modification with slight shift in some reflection positions, but the polymorphs remained the same since their d spacings were very close to those assigned to stable form of goat fat (Attama and Müller-Goymann, 2006). The slight shoulder observed for goat fat at $2\theta = 21.3°$, $d = 4.17$ Å was absent in the new lipid matrix after one month.

Reflections due to pure Phospholipon 90G® at $2\theta = 7.8°$, $d = 11.34$ Å (high intensity); $2\theta = 3.9°$, $d = 22.85$ Å; $2\theta = 6.5°$, $d = 13.60$ Å; $2\theta = 18.0°$, $d = 4.93$ Å (medium intensity); $2\theta = 16.3°$, $d = 5.44$ Å (low intensity) and $2\theta = 13.0°$, $d = 6.81$ Å; $2\theta = 14.7°$, $d = 6.03$ Å (weak intensity) were not reflected in the new lipid matrix (Fig. 3). The intensity of the reflection at $2\theta = 19.4°$, $d = 4.58$ Å in the new lipid matrix increased compared with the homolipid alone at $2\theta = 19.3°$, $d = 4.60$ Å.

WAXD diffractograms of the SLN are presented in Fig. 4 representing measurement after one month. The diffractograms all showed diffuse reflections 24 h after preparation (figure not shown). Liquid crystalline state of nanoparticles is usually reflected in the X-ray scattering pattern of diffuse nature in the wide-angle region (Kuntsche et al., 2004), and due to the highly disordered interior, Bragg reflections may not be

Table 1
Calculated lattice parameters for the templated homolipid

One day			One week			One month		
2θ (°)	d (Å)	Intensity (cts)	2θ (°)	d (Å)	Intensity (cts)	2θ (°)	d (Å)	Intensity (cts)
4.0	22.09	V. weak	4.0	22.09	Weak	4.0	22.09	Weak
6.0	14.73	V. high	6.0	14.73	V. high	6.0	14.73	V. high
10.0	8.85	V. weak	10.0	8.85	V. weak	10.0	8.85	V. weak
19.4	4.58	V. high	19.4	4.58	V. high	19.4	4.58	V. high
20.7	4.29	V. high	20.7	4.29	V. high	20.7	4.29	V. high
23.0	3.87	V. high	23.1	3.85	V. high	23.1	3.85	High

observed (Baraukas et al., 2005). However, after storage for one month WAXD plots for SLN3 and SLN4 showed very weak intensity reflections at $2\theta = 19.3^\circ$, $d = 4.60$ Å and $2\theta = 19.4^\circ$ $d = 4.58$ Å, respectively, and a very weak signal for SLN2 at $2\theta = 19.4^\circ$, $d = 4.58$ Å. These reflections were in β modification thus showing that there was no change in modification of the lipid matrix, but only a minor increase in crystallinity. Presence of these reflections also proved that particles were actually present but of low crystalline order as detected by DSC.

3.4. Particle size

Particle size is considered a major issue for pharmaceutical applications since it greatly influences in vitro and in vivo studies. The particle sizes obtained by static light scattering (Laser diffraction, LD-PIDS) are presented in Table 2. The particles were very small and characterized by absence of micrometer particles after one month. Melt-homogenization adopted for the production of these SLN have been shown to produce small particles for systems stabilized with phospholipids and non-ionic surfactants (Mehnert and Mäder, 2001). The result indicated that more than 90% of the particles were smaller than 0.377 μm after one month. The diameter $d_{90\%}$ is sensitive to the presence of a few large particles, and that means higher $d_{90\%}$ indicates the presence of micrometer particles and increases with increasing amount of these particles. The $d_{90\%}$ of the SLN were in the range of 0.152–0.377 μm within one month indicating very low amount of micrometer particles and a relatively narrow particle size distribution. It was observed that increase in polysorbate 80 concentration led to the decrease in particles size as a result of a decrease in interfacial tension and thus, an increase in the interfacial area (Schubert and Müller-Goymann, 2005). High concentration of emulsifier reduce the interfacial tension and facilitate particle disintegration during homogenisation. Also interesting was the fact that SLN formed without polysorbate 80 (SLN4) but had higher average particle size distribution compared with those containing polysorbate 80. Nanoparticle formation at 30% (w/w) lecithin without additional emulsifier has been reported however, not being stable yet (Schubert and Müller-Goymann, 2005). At each level of polysorbate 80 concentration, there was a slight growth in particle size after a period of one month evidenced by the increase in $d_{50\%}$, $d_{75\%}$ and $d_{90\%}$ values (Table 2). However, all the SLN remained in the lower nanometer range and were monodisperse with low standard deviations. The small increase in particle size observed for the dispersions may be related to the slight increase in the crystallinity of the particles present in these systems (Kuntsche et al., 2004). The physical stability of nanodispersions depends on particle size and particle size distribution. Appropriate control of particle size is needed to maximize the physical stability of dispersions. The applicability of SLN as oral, topical or parenteral drug delivery systems depends to a large extent on the particle size, particle size distribution and particle size stability. For instance, small and narrow distribution of particle size is required for parenteral administration while particles size distribution may not be a major issue for topical dosage forms. The particle size stability achieved in this formulation was as a result

Table 2
Particle sizes of the SLN

Batch	Mean volume distribution (μm ± S.D.)*									
	One day			One week			One month			
	$d_{50\%}$	$d_{75\%}$	$d_{90\%}$	$d_{50\%}$	$d_{75\%}$	$d_{90\%}$	$d_{50\%}$	$d_{75\%}$	$d_{90\%}$
SLN1	0.077 ± 0.005	0.092 ± 0.007	0.106 ± 0.009	0.072 ± 0.014	0.086 ± 0.022	0.117 ± 0.057	0.091 ± 0.011	0.122 ± 0.022	0.152 ± 0.011
SLN2	0.091 ± 0.003	0.113 ± 0.005	0.136 ± 0.006	0.093 ± 0.002	0.118 ± 0.003	0.145 ± 0.007	0.105 ± 0.007	0.139 ± 0.011	0.181 ± 0.022
SLN3	0.088 ± 0.003	0.112 ± 0.006	0.157 ± 0.009	0.093 ± 0.001	0.119 ± 0.002	0.159 ± 0.007	0.132 ± 0.008	0.193 ± 0.009	0.377 ± 0.014
SLN4	0.105 ± 0.007	0.124 ± 0.010	0.159 ± 0.011	0.094 ± 0.002	0.121 ± 0.012	0.169 ± 0.011	0.139 ± 0.007	0.209 ± 0.010	0.345 ± 0.022

SLN1-4 represent SLN formulated with 1.0, 0.5, 0.1 and 0.0% (w/w) of polysorbate 80, respectively.
* $n = 3$.

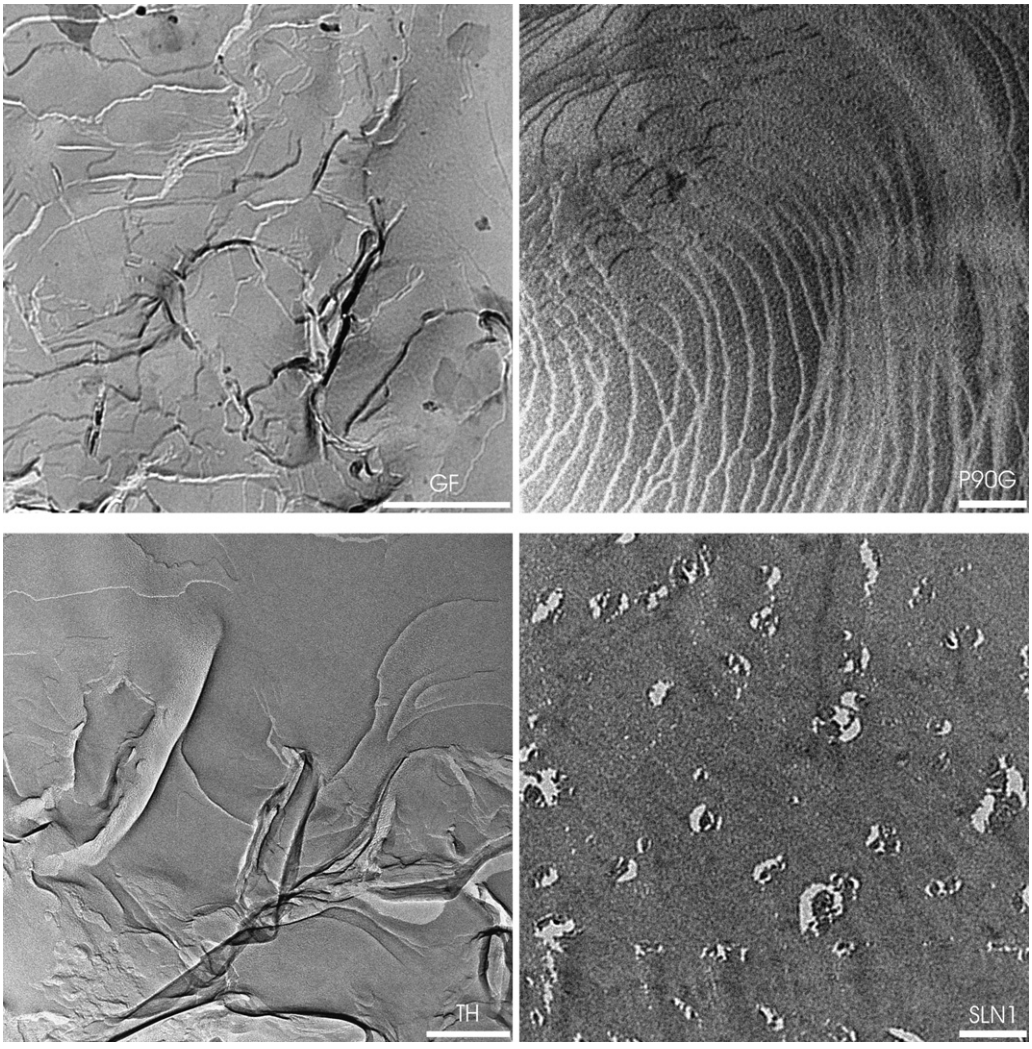

Fig. 5. FFTEM micrographs: homolipid (GF), Phospholipon 90G® (P90G), templated homolipid (TH), SLN containing 1.0% (w/w) ploysorbate 80 (SLN1). Bars represent 500, 200, 100 and 100 nm, respectively.

of the templation of the goat fat by the heterolipid (phospholipid), which resulted in the Phospholipon 90G® being anchored almost entirely on the nanoparticle surface, with polysorbate 80 providing further synergistic stabilization. Anchorage of Phospholipon 90G® on lipid surface has been noted to result in high negative zeta potential (Schubert and Müller-Goymann, 2005) and thus, stabilization by electrostatic phenomenon was also possible. Therefore, particle–particle interaction and subsequent agglomeration was greatly reduced. P90G and goat fat produced stable nanocarriers, which could be applied in different drug delivery systems. Unlike synthetic lipids, goat fat and P90G are natural lipids and the issue of in vivo toxicity is not a problem, and could be further engineered for intracellular drug delivery and targeting.

3.5. Freeze-fracture transmission electron microscopy

The FFTEM micrographs of the lipids, templated homolipid and SLN containing 1.0% (w/w) polysorbate 80 (SLN1) are presented in Fig. 5. The homolipid (goat fat) alone showed layered structures of triglycerides with less sharp edges representing the crystalline characteristics, while Phospholipon 90G® showed smooth lamellar sheets representing the mesomorphous characteristics. However, the templated homolipid showed smooth lamellar packing due possibly to a greater ordering of the homolipid. The FFTEM of the SLN1 showed defined anisometric structures with homogenous surface. It should be noted that particles align in three dimensions, whereas the micrographs only show two dimensional view of the particles. Hence, the given particle dimensions are only estimates due to the fact that a particle observation exactly top-on and edge-on, respectively, is rare and cannot be discriminated from slight particle twists, in addition. However, for this SLN, the particle size estimated from FFTEM micrograph is in consonance with values obtained from static light scattering measurements. Within the particles, layered structures such as terraces and steps being typical of crystalline solids were observed (Siekmann and Westesen, 1996). Thus, crystalline character of the SLN can be deduced. Although, this system contains high amount of lecithin (phospholipid), neither spherical particles with lamellar interfaces indicating liposome formation due to lecithin leakage during SLN preparation nor spherical multilayers surrounding a

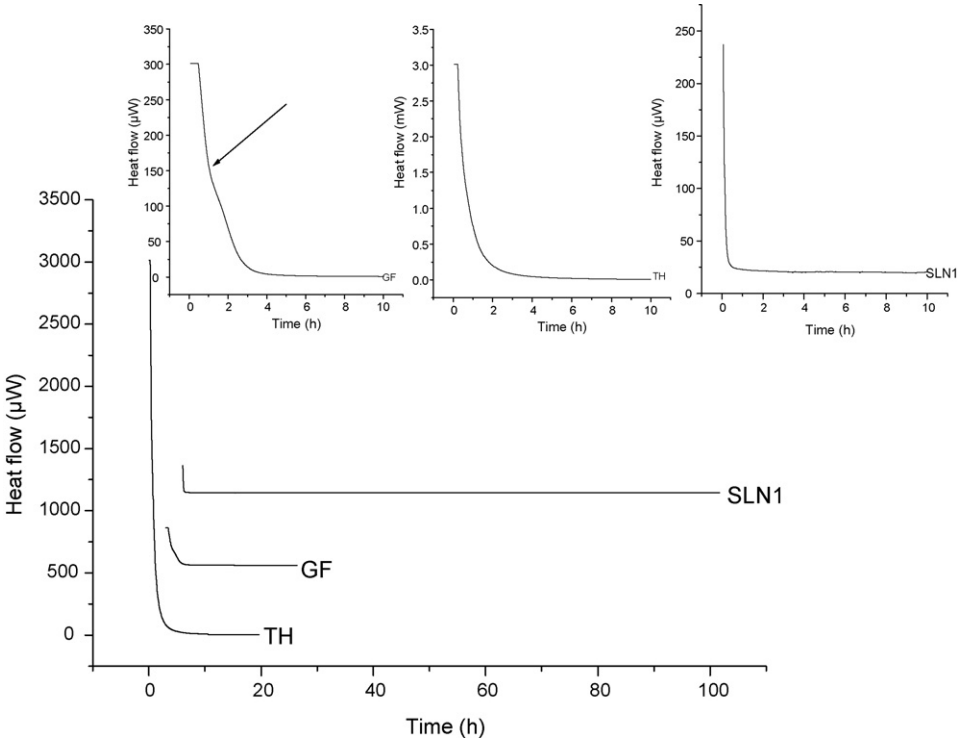

Fig. 6. Crystallization exotherms: homolipid (GF), templated homolipid (TH) and SLN containing 1.0% (w/w) polysorbate 80 (SLN1). Inset are the magnified single plots up to 10 h.

triglyceride core were observed (Schubert et al., 2006). The size and shape of a nanoparticle may also be influenced by the velocity of lipid crystallization, the lipid hydrophilicity (influence of self-emulsifying properties) and the shape of the lipid crystals and therefore, the surface area (Mehnert and Mäder, 2001). The shape of the nanoparticles may partly be related to the coarse crystal texture observed in the PLM of the templated homolipid after one month (Fig. 2).

3.6. Isothermal heat conduction microcalorimetry

Isothermal microcalorimetry can provide precise and rapid knowledge about possible solid state transition processes. Microcalorimetry is an analytical technique that has found numerous applications within the pharmaceutical environment especially in solid state pharmaceutics such as physical form characterization (Phipps and Mackin, 2000). Preformulation issues such as amorphicity and polymorphism can be assessed with ease, precision and confidence. The excellent sensitivity and long term baseline stability make it an ideal method for preformulation studies. In the context of lipid nanoparticle technology, studying the crystallization of SLN is necessary because it guides formulation scientists on when to carry out drug content analysis (encapsulation efficiency) of SLN or other lipidic systems prepared by melting and recrystallization. Previously encapsulated drug molecules may be partly expelled on complete recrystallization of lipidic systems.

The crystallization exotherms of the homolipid, templated homolipid, and SLN1 are presented in Fig. 6. There was a greater heat flow in the templated homolipid compared with the homolipid and SLN1. This may be due to the presence of Phospholipon 90G®. The most striking finding is a confirmation of templation detected in these exotherms, shown by the absence of change in crystallization behaviour of the exotherms of both the templated homolipid and SLN1. A change of slope was detected for the homolipid after about 45 min of isothermal crystallization (see arrow in inset, Fig. 6). This was attributed either to change in modification or change in crystal growth rate occasioned by completion of crystallization of the higher melting fraction of the homolipid (Attama and Müller-Goymann, 2006). SLN1 showed spontaneous crystallization without change in crystallization behaviour and the study of SLN1 was extended to 96 h to check if there could be any change in crystallization behaviour and nothing was detected. This means that templation by Phospholipon 90G® led to modification of crystallization of the lower melting fraction of the homolipid. Crystallization of SLN may be delayed and SLN may remain amorphous or supercooled for a very long time (Mehnert and Mäder, 2001). In this study, low crystalline SLN were obtained even after one month of storage as detected by DSC and WAXD measurements (Figs. 1b and 4). Since there was no change in crystallization behaviour of the SLN, assessment of some properties of the SLN within 24 h would give valid results.

Results of further analysis of the Avrami equation within the first 360 s of isothermal crystallization are presented in Fig. 7 and Table 3, representing plots of the normalized equation and kinetic parameters derived therefrom, respectively. The Avrami exponent n, which is indicative of the mechanism of nucleation were lower in SLN and templated homolipid compared

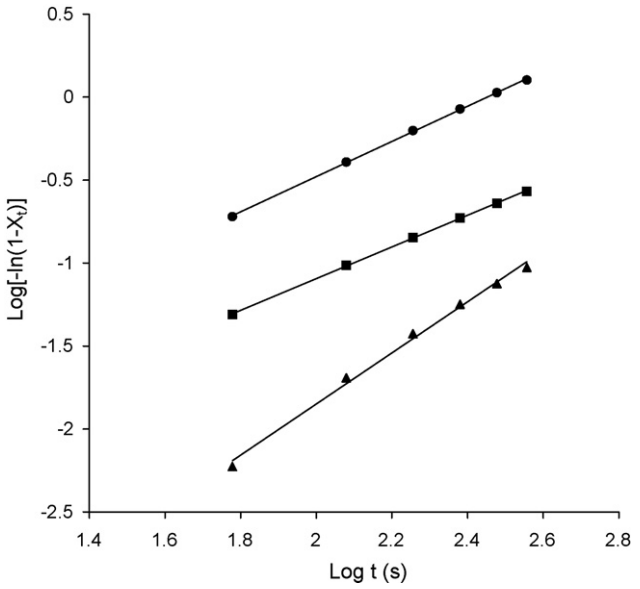

Fig. 7. Isothermal crystallization kinetic plots within the first 360 s of crystallization: (▲) homolipid, (■) templated homolipid, (●) SLN containing 1.0% (w/w) polysorbate 80 (SLN1).

Table 3
Isothermal crystallization parameters derived within first 360 s of isothermal crystallization

Batch	Parameter		
	n	k (s^{-1})	r^2
GF	1.5	1.18×10^{-5}	0.9950
TH	1.0	9.95×10^{-4}	0.9998
SLN1[a]	1.1	2.51×10^{-3}	0.9996

[a] Represents SLN containing 1% (w/w) polysorbate 80. GF (Homolipid), TH (templated homolipid), n = Avrami's exponent, k = crystal growth rate constant and r^2 = regression coefficient.

with the pure homolipid (Table 3). This means the templated homolipid and SLN1 possess similar nucleation mechanisms different from the pure homolipid. This result further lends proof to the fact that addition of Phospholipon 90G® exerted a templation effect on the homolipid (goat fat). The low values of n obtained also shows that one dimensional heterogeneous nucleation was the predominant process. Avrami exponent in the approximate range of ca. 2.0–2.9 suggests a two-dimensional growth from a combination of thermal and athermal nuclei (i.e. instantaneous and sporadic nucleation mechanisms) (Supaphol, 2001). The fractional values of n obtained show deviation from Avrami equation which specifies integral n values. Fractional n values and deviation from Avrami equation result from some assumptions made in the Avrami model such as constant growth rate, constant density and shape of growing nuclei, no change in volume during phase transformation among others (Avrami, 1941), which may not be easily obtainable in practice. The k values corresponding to the growth rates were higher in SLN and templated homolipid compared with the pure homolipid indicating templation favoured the crystallization process.

4. Conclusion

The templating effect led to the disappearance of the lower melting peak and did not significantly affect the higher melting peak of the homolipid (goat fat), but affected the total enthalpy of the endothermic process. This is a very useful finding as lipid matrix with a more cooperative thermal phase transition with less crystallinity resulted. SLN formulated with this lipid matrix were also of low crystallinity and did not show change in crystallization behaviour. As a result, very stable nano-sized particles were produced, which could be further engineered for use in parenteral or ocular drug delivery, or in other targeted drug delivery systems (active or passive targeting), as the component lipids are highly biocompatible. SLN containing 1.0% polysorbate 80 possessed the best qualities. The result of this study also shows a method of improving natural lipids for use in particulate drug delivery systems. This finding will elicit further researches using natural lipids as search for ideal drug delivery system for drugs continues.

Acknowledgements

This work is a product of research fellowship awarded by Alexander von Humboldt Stiftung. Dr. A.A. Attama wishes to acknowledge the support (Ref. No. IV-NRI/1112681 STP). We also thank Phospholipid GmbH, Köln for providing materials.

References

Attama, A.A., Müller-Goymann, C.C., 2006. A critical study of physically structured lipid matrices composed of a homolipid from *Capra hircus* and theobroma oil. Int. J. Pharm. 322, 67–78.

Attama, A.A., Nkemnele, M.O., 2005. In vitro evaluation of drug release from self micro-emulsifying drug delivery systems using a biodegradable homolipid from *Capra hircus*. Int. J. Pharm. 304, 4–10.

Attama, A.A., Nzekwe, I.T., Nnamani, P.O., Adikwu, M.U., Onugu, O.C., 2003. The use of solid self emulsifying systems in the delivery of diclofenac. Int. J. Pharm. 262, 23–28.

Avrami, M., 1939. Kinetics of phase change. I. General theory. J. Chem. Phys. 7, 1103–1112.

Avrami, M., 1940. Kinetics of phase change. II. Transformation–time relations for random distribution of nuclei. J. Chem. Phys. 8, 212–224.

Avrami, M., 1941. Kinetics of phase change. III. Granulation, phase change and microstructure. J. Chem. Phys. 9, 177–184.

Baraukas, J., Johnsson, M., Tiberg, F., 2005. Self-assembled lipid superstructures: beyond vesicles and liposomes. Nano Lett. 5, 1615–1619.

Bunjes, H., Koch, M.H.J., 2005. Saturated phospholipids promote crystallization but slow down polymorphic transition in triglyceride nanoparticles. J. Control. Rel. 107, 229–243.

Cortesi, R., Nastruzzi, C., 2001. Delivery systems for DNA-binding drugs as gene expression modulators. Drug Deliv. Today 6, 893–904.

Ghyczy, M., Niemann, R., 1992. Wissenschaftliche Publikation, Haut und Liposomen, vol. 1. Nattermann Phospholipid GmbH.

Hou, D.-Z., Xie, C.-S., Huang, K.-J., Zhu, C.-H., 2003. The production and characterization of solid lipid nanoparticles (SLNs). Biomaterials 24, 1781–1785.

Kuntsche, J., Westesen, K., Drechsler, M., Koch, M.H.J., Bunjes, H., 2004. Supercooled smectic nanoparticles: a potential novel carrier system for poorly water soluble drugs. Pharm. Res. 21, 1834–1843.

Mehnert, W., Mäder, K., 2001. Solid lipid nanoparticles production, characterization and applications. Adv. Drug Deliv. Rev. 47, 165–196.

Müller, R.H., Mäder, K., Gohla, S., 2000. Solid lipid nanoparticles (SLN) for controlled drug delivery—a review of the state of the art. Eur. J. Pharm. Biopharm. 50, 161–177.

Panyam, J., Labhasetwar, V., 2004. Sustained cytoplasmic delivery of drugs with intracellular receptors using biodegradable nanoparticles. Mol. Pharm. 1, 77–84.

Panyam, J., Zhou, W.-Z., Prabha, S., Sahoo, S.K., Labhasetwar, V., 2002. Rapid endolysosomal escape of poly (DL-lactide-co-glycolide) nanoparticles: implications for drug and gene delivery. Faseb J. 16, 1217–1226.

Phipps, M.A., Mackin, L.A., 2000. Application of isothermal microcalorimetry in solid state drug development. Pharm. Sci. Technol. Today 3, 9–17.

Radtke, M., Souto, E.B., Müller, R.H., 2005. Nanostructured lipid carriers: a novel generation of solid lipid drug carriers. Pharm. Tech. Europe 17, 45–50.

Sastry, M., 2000. Nanostructured thin films by self-assembly of surface modified colloidal particles. Curr. Sci. 78, 1089–1097.

Schubert, M.A., Meike, H., Müller-Goymann, C.C., 2006. Structural investigations on lipid nanoparticles containing high amounts of lecithin. Eur. J. Pharm. Sci. 27, 26–236.

Schubert, M.A., Müller-Goymann, C.C., 2005. Characterization of surface-modified solid lipid nanoparticles (SLN): influence of lecithin and non-ionic emulsifier. Eur. J. Pharm. Biopharm. 61, 77–86.

Schubert, M.A., Müller-Goymann, C.C., 2003. Solvent injection as a new approach for manufacturing lipid nanoparticles—evaluation of the method and process parameters. Eur. J. Pharm. Biopharm. 55, 125–131.

Schubert, M.A., Schicke, B.C., Müller-Goymann, C.C., 2005. Thermal analysis of the crystallization and behaviour of lipid matrices and lipid nanoparticles containing high amounts of lecithin. Int. J. Pharm. 298, 242–254.

Siekmann, B., Westesen, K., 1996. Investigation on solid lipid nanoparticles prepared by precipitation in o/w emulsions. Eur. J. Pharm. Biopharm. 43, 104–109.

Siekmann, B., Westesen, K., 1992. Sub-micron sized parenteral carrier systems based on solid lipid. Pharm. Pharmacol. Lett. 1, 123–126.

Stuchlík, M., Žák, S., 2001. Lipid based vehicle for oral drug delivery. Biomed. Papers 145, 17–26.

Supaphol, P., 2001. Application of the Avrami, Tobin, Malkin, and Urbanovici-Segal macrokinetic models for isothermal crystallization of syndiotactic polypropylene. Thermochim. Acta 370, 37–48.

Westesen, K., Bunjes, H., Koch, M.H.J., 1997. Physicochemical characterization of lipid nanoparticles and evaluation of their drug loading capacity and sustained release potential. J. Control. Rel. 48, 189–197.

Westesen, K., Bunjes, H., Koch, M.H.J., 2003. Influence of emulsifiers on the crystallization of solid lipid nanoparticles. J. Pharm. Sci. 92, 1509–1520.